Heliyon 10 (2024) e25575

Contents lists available at ScienceDirect

Heliyon

journal homepage: www.cell.com/heliyon

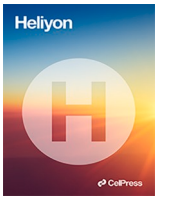

Research article

# Selective lithium extraction from spent lithium-ion batteries through polyvinyl chloride thermal decomposition-based gas-solid reaction

Biyuan Yang [a,**], Xinyu Lu [b], Xiaowei Wang [b,*], Jiafeng Zhang [b]

[a] Hunan Prevention and Treatment Institute for Occupational Diseases, Changsha, 410007, PR China
[b] National Engineering Laboratory for High-efficiency Recovery of Refractory Nonferrous Metals, School of Metallurgy and Environment, Central South University, Changsha, 410083, PR China

ARTICLE INFO

*Keywords:*
Spent lihtiun ion batteries
Selective lithium extraction
Gas-solid reaction
Polyvinyl chloride

ABSTRACT

The recovery of valuable metals from waste battery materials and the thermal decomposition of PVC both require significant energy and material consumption. In this study, we propose an innovative strategy that integrates the lithium extraction process from spent $LiNi_{0.85}Co_{0.15}Al_{0.05}O_2$ (S-NCA) with PVC pyrolysis, resulting in a substantial reduction in energy consumption and chemical additive. Various characterization techniques, including SEM, TEM, XRD, and XPS, are employed to investigate the mechanism of gas-solid lithium extraction and provide valuable insights into the migration pathway of lithium from S-NCA to soluble LiCl. The optimal conditions for the process were determined as follows: a temperature of 600 °C, S-NCA/PVC mass ratio of 1:4, and a baking time of 2 h, achieving a lithium extraction efficiency of 94.37 %. The research provides valuable insights for the valorization of PVC thermal decomposition and lithium extraction from NCA, presenting a novel approach for future applications.

## 1. Introduction

Energy serves as a crucial pillar for human societal development, providing convenience, and efficiency, and driving continuous progress [1,2]. While traditional fossil fuels have been the primary energy source, their depletion and associated environmental impacts have necessitated the exploration of greener and more sustainable alternatives [3,4]. Renewable energy sources such as geothermal, wind, and solar power have emerged as viable options due to their wide availability and environmental friendliness [5–9]. However, their intermittent nature requires the development of efficient energy storage systems. Among these systems, lithium-ion batteries have gained prominence due to their high energy density, low self-discharge rate, and extended lifespan [10,11].

With the rapid advancement of energy storage technology and the widespread adoption of electric vehicles, the demand for metals like nickel (Ni), cobalt (Co), and manganese (Mn) has surged worldwide [12,13]. Lithium (Li), a critical component of lithium-ion batteries [14,15], has experienced a significant increase in price as a result [16,17]. To address this challenge and maximize the utilization of secondary resources, the recycling of waste lithium batteries has gained immense strategic importance [18,19]. Currently, research on selective lithium extraction predominantly centers around $LiFePO_4$ due to its inherent value. However, the

* Corresponding author.
** Corresponding author.
*E-mail addresses:* 434698152@qq.com (B. Yang), yjywxw@csu.edu.cn (X. Wang).

https://doi.org/10.1016/j.heliyon.2024.e25575
Received 6 October 2023; Received in revised form 25 January 2024; Accepted 30 January 2024
Available online 5 February 2024

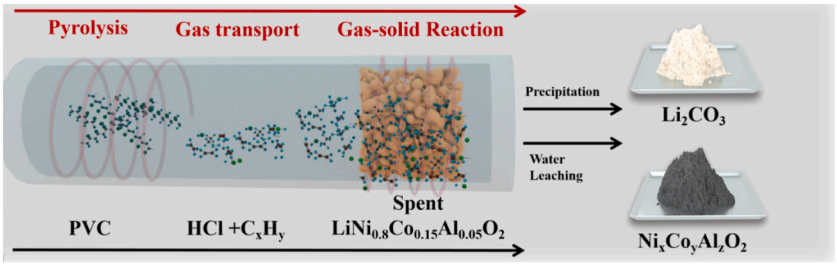


**Fig. 1.** Flowchart illustrating the recovery process of S-NCA batteries through a PVC thermal decomposition-based gas-solid reaction.

selective extraction of lithium from ternary lithium-ion cathode materials lags behind that of $LiFePO_4$. Previous studies by Kong et al. [20] employed NaClO as a reducing agent for selective Li leaching in an acidic HCl environment, while Ma et al. [21] utilized ethylene glycol for selective Li separation in a supercritical water system, yielding promising results. Despite these achievements, the scalability and practicality of these methods remain open for discussion.

The HCl system encounters significant challenges related to equipment corrosion during acid leaching, and the use of ethylene glycol and ultra-pure water systems in Ma et al.'s approach raises concerns about increased recovery process costs. Zhang et al. [22] proposed a study involving roasting and recovering Li from $LiNi_xCo_yMn_zO_2$ in a $CH_4$ atmosphere, successfully generating LiCO3, NiO, CoO, and MnO, effectively separating lithium. However, the use of $CH_4$ poses inherent dangers, potentially leading to explosion risks during the roasting process.

This manuscript focuses on the integration of waste lithium battery metal recovery with the thermal decomposition process of PVC. PVC, a widely used plastic material, poses significant challenges in terms of disposal and recycling due to its abundant chlorine content [20–22]. During the thermal decomposition of PVC, the chlorine is converted into hydrogen chloride (HCl) gas [23,24]. In this study, we propose leveraging the generated HCl to achieve efficient and selective lithium extraction from waste lithium batteries, thereby reducing overall recycling costs.

The integration of waste lithium battery metal recovery with PVC thermal decomposition presents a promising solution to address two pressing issues simultaneously: the proper disposal of PVC waste and the efficient recovery of valuable metals from waste lithium batteries. By combining these processes, we aim to capitalize on the environmental benefits of green energy sources while promoting a circular economy in the battery industry [25]. This manuscript explores the potential of this integrated approach and discusses its implications for achieving a more sustainable and cost-effective recycling system by applying the HCl generated from polyvinyl chloride thermal decomposition. Overall, this study contributes to the ongoing efforts to bridge the gap between energy demand, resource scarcity, and environmental preservation, paving the way for a more sustainable and efficient future.

## 2. Experimental section

### 2.1. Material synthesis

All reagents were purchased from Sinopharm Chemical Reagent Limited corporation (analytical reagent). Spent S-NCA electrodes attached to current collector aluminum foil were obtained from Zhejiang Huayou Cobalt Co., Ltd (Zhejiang, China). A predetermined quantity of S-NCA was thoroughly mixed with PVC using a planetary ball mill to ensure homogeneity. Subsequently, batches of 5g of the mixture were subjected to roasting in a muffle furnace in the air atmosphere with a heating rate of 5 °C/min, while the generated gases were efficiently absorbed by the fume hood ventilation system. Following roasting, the resulting product underwent water leaching in deionized water at a controlled temperature of 60 °C, and subsequent analysis allowed for the determination of elemental concentrations during the leaching process. The brand of the Muffle furnace is Kejing, the model is KSL-1100X, and the furnace body size is (130*100*100 mm). After the leaching, the residue is collected and the lithium-rich solution is used for the subsequent lithium deposition step.

The leaching rate of the metal in S is calculated by eq (1):

$$\eta_s = \frac{c_s \times V}{m_s \times \omega_s} \times 100\% \tag{1}$$

Where $\eta_s$ represents the leaching efficiency of the "s" element, $m_s$ and $\omega_s$ are the mass of the S-NCA and the content of element "s" in it, $c_s$ and $V$ is the concentration of element "s" and volume of the leaching solution.

### 2.2. Material characterization

The X-ray diffraction (XRD, 2Empyrean 2, PANalytical) spectroscopy technique was employed to investigate the structural evolution of the material. The microstructure and elemental distribution of the reaction were examined using scanning electron microscopy (SEM, JSM-6360LV, JEO), transmission electron microscopy (TEM), and energy-dispersive X-ray spectroscopy (EDS). Quantitative measurements of the precursor composition were conducted using inductively coupled plasma-optical emission

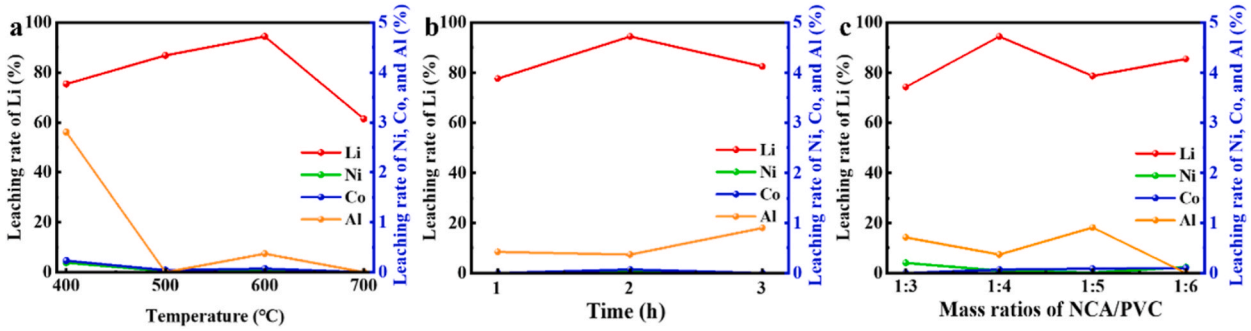


**Fig. 2.** **a** Li leaching rates at different roasting temperatures (m(S-NCA)/m(PVC) ratio is 1:4, and reaction time is 2 h); **b** Li leaching rates at different roasting time (m(S-NCA)/m(PVC) ratio is 1:4, and temperature is 600 °C); **c** Li leaching rate at different m(S-NCA)/m(PVC) ratios (reaction time is 2 h, and temperature is 600 °C).

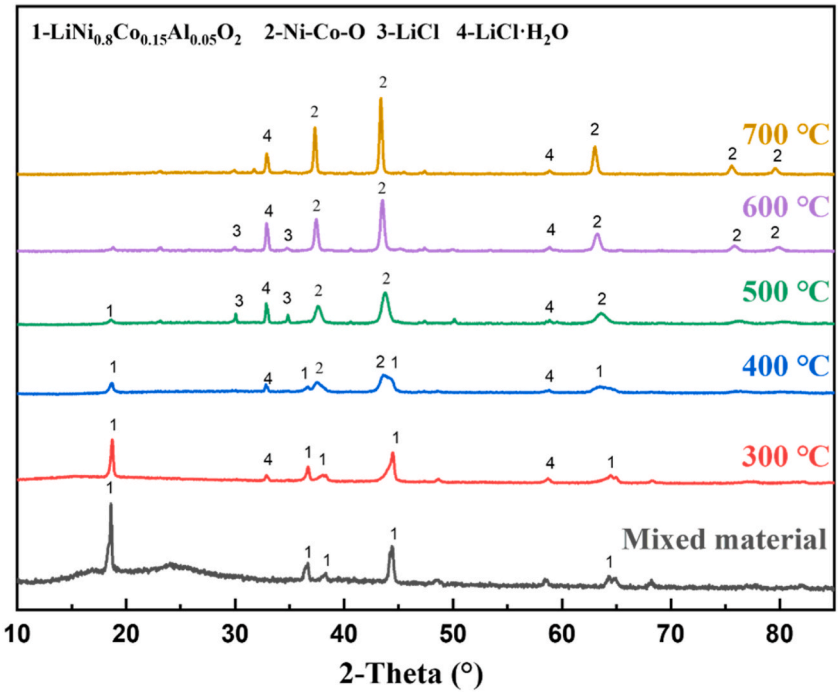


**Fig. 3.** XRD patterns of the mixture and products after roasting at various temperatures (300–700 °C).

spectrometry (ICP-OES) with the ICAP7400 radial instrument from Thermo Fisher. The valence state of the elements was characterized by X-ray photoelectron spectroscopy (XPS, Thermo Fisher Scientific K-Alpha, China).

## 3. Results and discussion

Based on the process schematic of the lithium extraction reaction through PVC thermal decomposition synergy, as shown in Fig. 1, PVC decomposes into HCl and hydrocarbon compounds during the heating process. Among them, HCl reacts with NCA under heating conditions, generating soluble lithium salts and oxides. Further separation of nickel-cobalt-aluminum oxides and lithium carbonate can be achieved through water leaching and sodium carbonate precipitation.

The recovery rate of various metals is an important indicator in the metal recovery process. Due to the formation of soluble lithium salts and insoluble oxides when S-NCA is mixed with PVC during roasting, the mixture can be separated through water leaching. Therefore, the recovery rates of various metal elements under different experimental conditions were studied. Firstly, the leaching rates of Li, Ni, Co, and Al at temperatures ranging from 400 to 700 °C are shown in Fig. 2a. As the temperature increases from 400 °C to 600 °C, the leaching rate of Li increases from 75.36 % to 94.37 %. However, as the temperature continues to rise to 700 °C, the leaching rate of Li decreases significantly. This may be due to the loss of Li caused by other components of PVC decomposition being carried into the air. At all temperatures, the leaching rates of Ni, Co, and Al remain low, so 600 °C was chosen as the roasting temperature for S-NCA

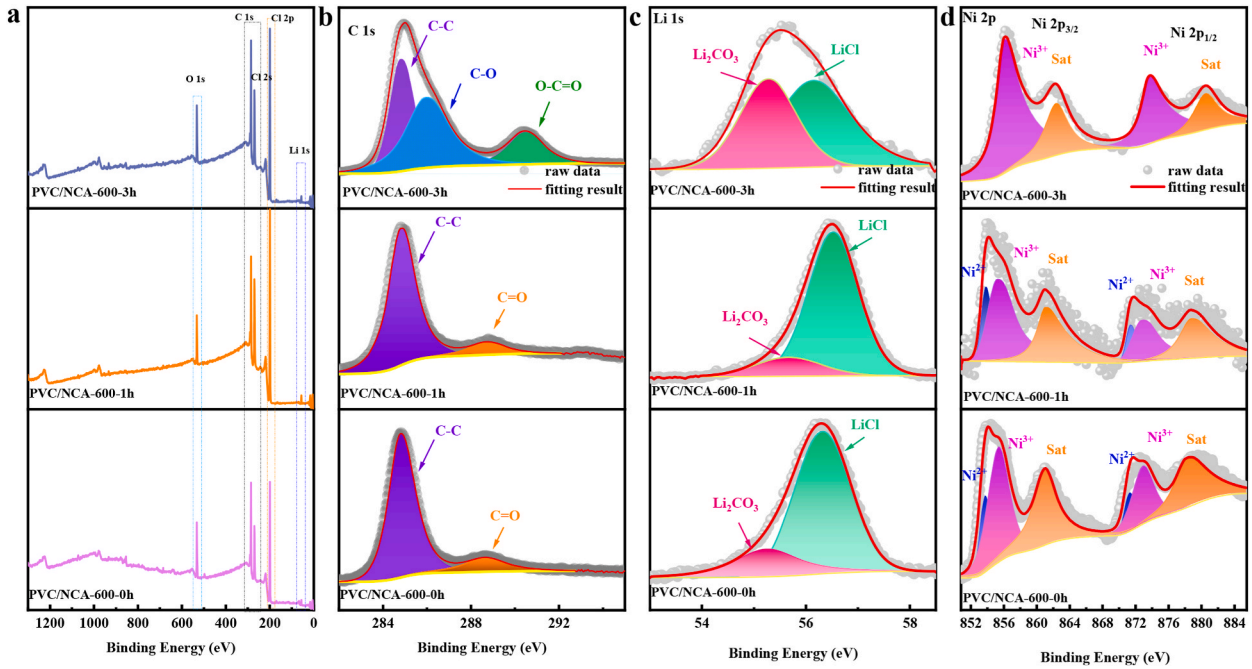


**Fig. 4.** XPS spectra of products reacted at 600 °C for 0, 1, 3 h **a** Survey spectra; **b** high-resolution C 1s spectra; **c** high-resolution Li 1s spectra; **d** high-resolution Ni 2p spectra.

and PVC.

In traditional roasting experiments, longer roasting time can achieve better results. However, considering energy consumption and time costs, it is necessary to explore the shortest roasting time. The results at different roasting times are shown in Fig. 2b. When the roasting time increases from 1 h to 3 h, the leaching rate of Li reaches its maximum at 2 h. The low leaching rate of Li at 1 h can be attributed to an incomplete reaction, while the Li loss at 3 h is not due to an incomplete reaction. Based on the above conditions, the optimal roasting conditions for PVC and S-NCA can be determined as follows: temperature of 600 °C, S-NCA/PVC mass ratio of 1:4, and roasting time of 2 h.

Furthermore, the mass ratio of the mixed raw materials will greatly determine the leaching rates of the metal elements. The roasting experiments were conducted with different mass ratios of the two raw materials. The relevant data are shown in Fig. 2c. Interestingly, the leaching rate of Li shows a peculiar trend. When the mass ratio of S-NCA: PVC increases from 1:3 to 1:4, the leaching rate of Li increases significantly. However, as the proportion of PVC continues to increase, the leaching rate of Li decreases. This can be attributed to the excess gas produced by PVC decomposition carrying away some Li. The leaching rates of Ni, Co, and Al are very low in the leaching process. The S-NCA/PVC mass ratio of 1:4 is economical and practical.

In order to study the phase transformation of S-NCA during roasting, XRD analysis was performed on the roasting products at different temperatures. From Fig. 3, it is clear that the peak of S-NCA is evident under the roasting condition of 300 °C, and a small amount of LiCl is formed, indicating that the structure of S-NCA is not destroyed at this temperature. Since LiCl easily absorbs moisture from the air, a portion of LiCl in the roasting product may exist in the form of $LiCl{\cdot}H_2O$. When the temperature rises to 400 °C, the intensity of the NCA characteristic peak decreases, and NiO phase gradually forms. In previous studies [26,27], the reduction of NCM was followed by the formation of NiO, indicating that the experiment was successful. In addition, since the raw material used is $LiNi_{0.8}Co_{0.15}Al_{0.05}O_2$, the generated product is mainly NiO and contains a small amount of Co, so Ni–Co–O is used instead in this paper [27].

At a roasting temperature of 500 °C, the NCA peak becomes weaker, and the peaks of LiCl and NiO begin to appear. This suggests that further decomposition and phase transformation of S-NCA have occurred, resulting in the formation of lithium carbonate and cobalt oxide compounds. As the temperature reaches 600 °C, the S-NCA peak disappears completely, indicating complete decomposition of S-NCA. The major phases observed in the roasting product are $LiCl{\cdot}H_2O$, LiCl, and NiO. This confirms the successful conversion of S-NCA into lithium carbonate and cobalt-nickel oxides under these conditions. Additionally, the XRD analysis of the roasting product at 600 °C shows the absence of PVC-related peaks, indicating that PVC has been completely decomposed and eliminated during the heating process. This further supports the efficiency of the PVC thermal decomposition synergy method for lithium extraction. The possible reaction is as follows:

$$LiNi_xCo_yAl_zO_2 + (CHCl - CH_2)_n + O_2 \rightarrow LiCl + Ni_xCo_yAl_zO + C_xH_yO_z$$

To gain insights into the elemental transformations during the S-NCA and PVC roasting process, X-ray Photoelectron Spectroscopy (XPS) analysis was conducted under the optimal conditions, except for the variation in roasting time. The temperature was set at

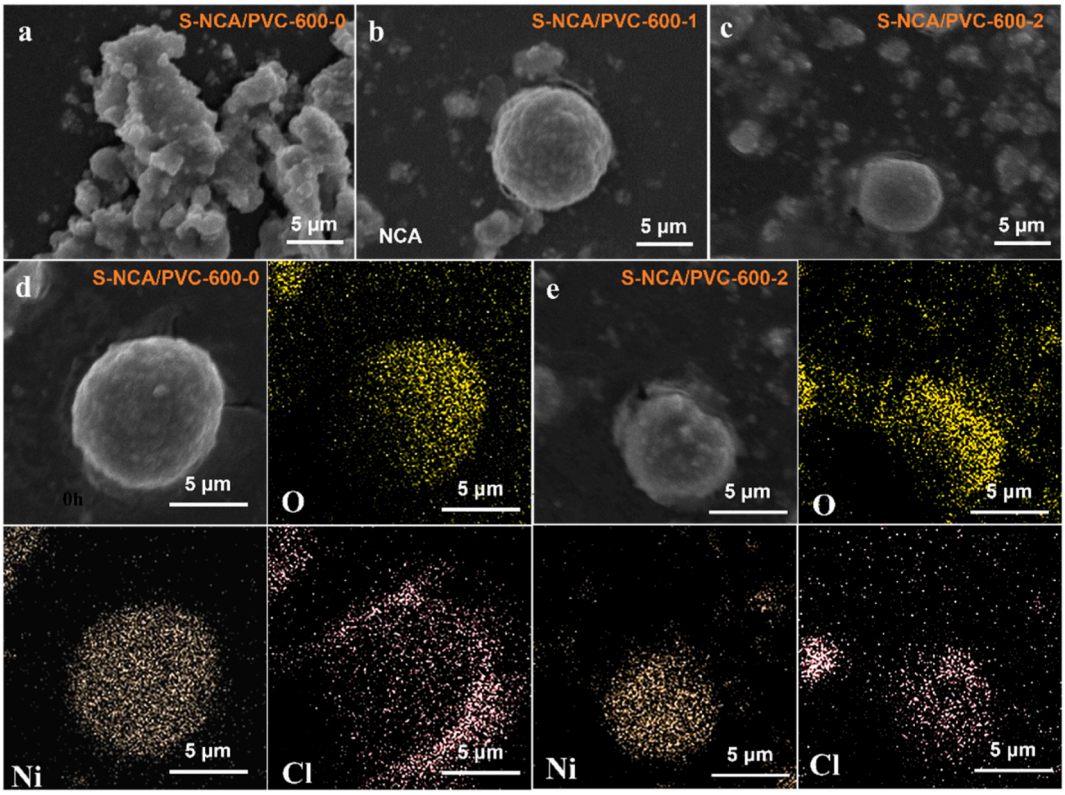


**Fig. 5.** SEM images of the S-NCA/PVC mixture reacted at 600 °C for 0 h **a**, 1 h **b**, and 2 h **c**; corresponding SEM-based EDS mapping images of O, Ni, and Cl elements of S-NCA/PVC mixture reacted at 600 °C for 0 h **d** and 2 h **e**.

600 °C, and the duration was varied from 0 h to 3 h to elucidate the reaction mechanism more effectively. Fig. 4a presents the XPS full spectra of different reaction stages, highlighting the corresponding characteristic peaks of O 1s, C 1s, Cl 2p, and Li 1s, confirming the release of lithium species. The carbon signals primarily arise from the deposition of carbonaceous compounds.

Further analysis focused on three key elements: Li, C, and Ni. The C 1s spectra revealed the presence of C═O chemical bonds at 288.66 eV, with respective contents of 13.79 %, 10.71 %, and 9.09 % at 0, 1, and 2 h (Fig. 4b). However, after 3 h of roasting, the C═O peak disappeared, replaced by C–O and O–C═O, indicating the formation of carbonate compounds on the product surface. In the case of Li, the Li 1s spectra indicated the presence of a small amount of $Li_2CO_3$ on the product surface during the 0–2 h process, accounting for approximately 14 % of the total Li species. This suggests that the initial form of lithium is LiCl. However, with an extended roasting time of 3 h, there was a noticeable change in the $Li_2CO_3$-to-LiCl ratio, with $Li_2CO_3$ occupying approximately 56.82 % of the total Li species. This increase can be attributed to the evaporation of LiCl and its subsequent conversion into $Li_2CO_3$, which aligns with the results obtained from the 3-h leaching process (Fig. 4c). Moreover, the leaching rate of Al exhibited a slight increase after 3 h of roasting. This finding suggests a possible reaction equation (2):

$$6LiCl + 3C + Al_2O_3 + 3O_2 = 3Li_2CO_3 + 2AlCl_3 \quad (2)$$

In the case of Ni, the Ni 2p spectra revealed an increasing content of $Ni^{2+}$ on the product surface with prolonged roasting time, from an initial content of 23.07 %–64.52 % (Fig. 4d). This indicates the transformation of Ni species in NCA to NiO during the roasting process. After 3 h, almost all Ni on the product surface existed as $Ni^{3+}$, which can be attributed to the oxidation of NiO to $Ni^{3+}$ over an extended duration in an air atmosphere. These results further support the understanding of the transformation mechanism during the roasting process (Fig. 4d).

SEM analysis was performed on the products obtained after 0 h and 2 h of roasting at 600 °C under the optimized conditions. The SEM images revealed significant particle fragmentation in the S-NCA particles during the initial stage of roasting (0 h) (Fig. 5a). However, at 1h, spherical S-NCA particles with good uniformity were observed, indicating that the reaction between S-NCA and PVC caused structural damage to some NCA particles, while others retained their original morphology, which is advantageous for subsequent reuse (Fig. 5b and c). The SEM analysis of the products after 2 h of roasting displayed a large number of intact spherical NCA particles (Fig. 5c). EDS mapping further conform the existence of Ni, Cl, and O at different reaction time (Fig. 5d and e).

The combustion products at 0 h and 2 h were subjected to TEM analysis to examine their microstructure. Prior to TEM analysis, a dispersion process was applied, leading to the detachment of substances adhering to particle surfaces while retaining a small amount. In the 0h product images, the main body comprises NiO, with a pasty LiCl layer on the surface. Focusing on this region causes the LiCl

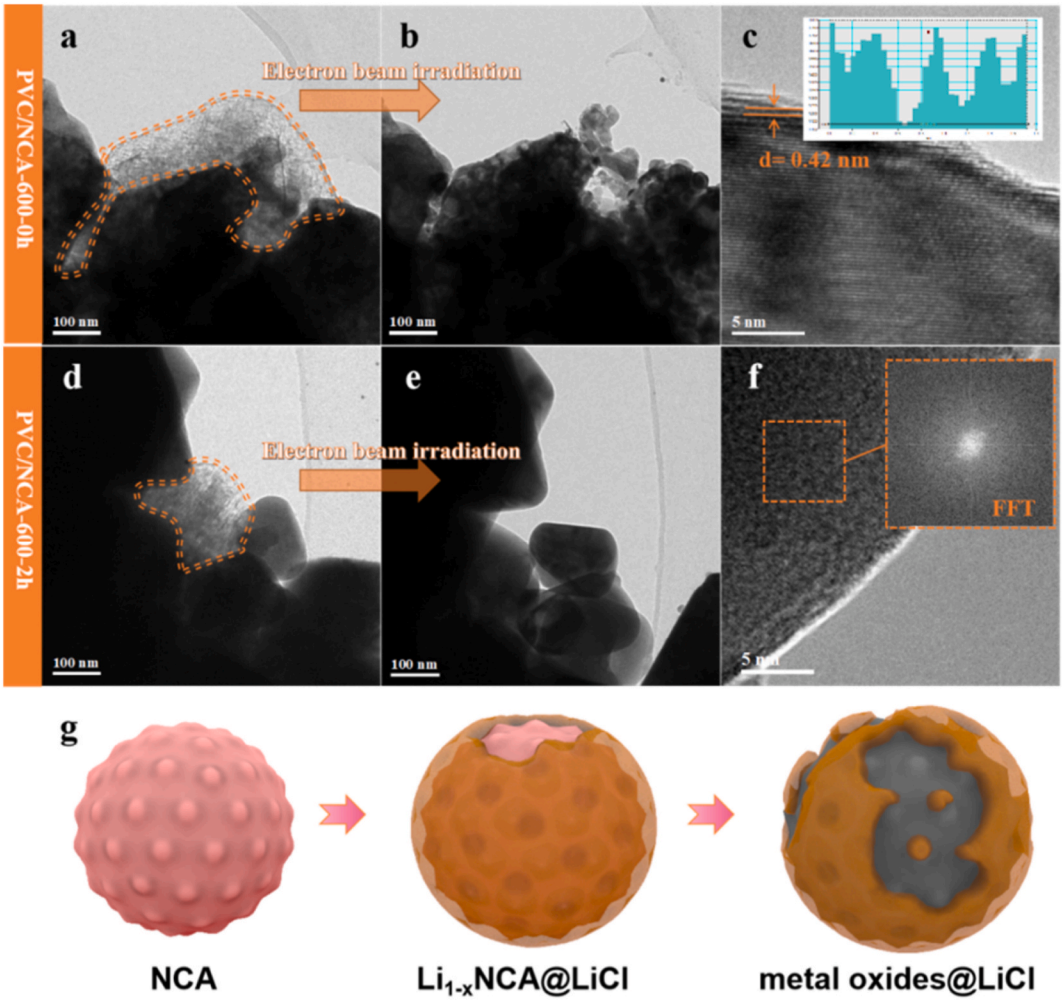


**Fig. 6.** Images before **a** and after **b** TEM electron etching of products reacted at 600 °C for 0 h; **c** high-resolution TEM image of the products reacted at 600 °C for 0 h; images before **d** and after **s** TEM electron etching of products reacted at 600 °C for 2 h; **f** high-resolution TEM image of the products reacted at 600 °C for 0 h; **g** mechanical diagram for $Li^+$ extraction from S-NCA under PVC roasting.

substance to disappear (Fig. 6a and b). HRTEM at the particle edges reveals clear lattice fringes with a spacing of 0.42 nm, corresponding to the (003) crystal plane of NMA that has not undergone lithium removal (Fig. 6c). After a 2 h reaction, the decomposition of the peripheral LiCl phase during the shooting process was similarly observed (Fig. 6d, **e**). Simultaneously, high-resolution images of the particles show the absence of distinct (003) crystal planes, indicating a more thorough lithium removal reaction (Fig. 6f). Combining SEM analysis, a plausible lithium removal mechanism was proposed (Fig. 6g). In the heating environment, the decomposed HCl reacts with NCA in a gas-solid reaction. Lithium gradually leaches out from the lattice, forming a thermodynamically stable LiCl phase on the surface, ultimately resulting in nickel-cobalt-aluminum oxide enveloped by LiCl.

Overall, the XPS, SEM, EDS, and TEM analyses provided valuable insights into the elemental transformations and morphological changes occurring during the S-NCA and PVC roasting process. These findings contribute to a better understanding of the reaction mechanism and offer guidance for optimizing the process conditions and product quality.

## 4. Conclusion

In conclusion, this study proposed a selective lithium extraction strategy using PVC plastic pyrolysis atmosphere. The efficient and selective lithium leaching was achieved by utilizing the HCl gas generated from PVC pyrolysis in a gas-solid reaction with S-NCA material. The gas-solid lithium extraction mechanism was elucidated through SEM, TEM, XRD, XPS, and EDS characterizations at different reaction stages. Under the optimized conditions of a roasting temperature of 600 °C, S-NCA/PVC mass ratio of 1:4, and a roasting time of 2 h, a lithium extraction efficiency of 94.37 % was achieved. This work provides a novel approach for the valorization of PVC pyrolysis and lithium extraction from S-NCA, opening up new avenues for future research in these areas.

## Additional information

No additional information is available for this paper.

## Data availability statement

| Question | Response |
|---|---|
| **Data Availability**<br>Sharing research data helps other researchers evaluate your findings, build on your work and to increase trust in your article. We encourage all our authors to make as much of their data publicly available as reasonably possible. Please note that your response to the following questions regarding the public data availability and the reasons for potentially not making data available will be available alongside your article upon publication. Has data associated with your study been deposited into a publicly available repository? | No |
| Please select why. Please note that this statement will be available alongside your article upon publication.<br>as follow-up to "**Data Availability**<br>Sharing research data helps other researchers evaluate your findings, build on your work and to increase trust in your article. We encourage all our authors to make as much of their data publicly available as reasonably possible. Please note that your response to the following questions regarding the public data availability and the reasons for potentially not making data available will be available alongside your article upon publication.<br>Has data associated with your study been deposited into a publicly available repository? | Data will be made available on request |

## CRediT authorship contribution statement

**Biyuan Yang:** Writing – original draft, Resources, Methodology, Investigation. **Xinyu Lu:** Software. **Xiaowei Wang:** Writing – review & editing, Supervision, Project administration, Investigation, Funding acquisition. **Jiafeng Zhang:** Writing – review & editing, Supervision, Project administration, Funding acquisition.

## Declaration of competing interest

The authors declare that they have no known competing financial interests or personal relationships that could have appeared to influence the work reported in this paper.

## Acknowledgments

We gratefully acknowledge the financial support from the National Natural Science Foundation of China (51902347 and 52202338).

## References

[1] H. Neofytou, A. Nikas, H. Doukas, Sustainable energy transition readiness: a multicriteria assessment index, Renew. Sustain. Energy Rev. 131 (2020) 109988, https://doi.org/10.1016/j.rser.2020.109988.
[2] J. Tollefson, Can the world kick its fossil-fuel addiction fast enough, Nature 556 (7702) (2018) 422–425, https://doi.org/10.1038/d41586-018-04931-6.
[3] J. Zhang, D. Peng, X. Gao, J. Zou, L. Ye, G. Ji, B. Luo, G. Yu, P. Li, X. Wang, Z. Zhao, B. Zhang, W. Hu, Z. Liu, L. Cheng, R. Zhao, Regeneration of high-performance materials for electrochemical energy storage from assorted solid waste: a review, J. Clean. Prod. 416 (2023) 137628, https://doi.org/10.1016/j.jclepro.2023.137628.
[4] X. Zhang, M. Ou, Y. Song, X. Li, Review of Middle East energy interconnection development, Journal of Modern Power Systems and Clean Energy 5 (2017) 917–935, https://doi.org/10.1007/s40565-017-0335-7.
[5] A. Osman, L. Chen, M. Yang, G. Msigwa, M. Farghali, S. Fawzy, D. Rooney, P. Yap, Cost, environmental impact, and resilience of renewable energy under a changing climate: a review, Environ. Chem. Lett. 21 (2022) 741–764, https://doi.org/10.1007/s10311-022-01532-8.
[6] X. Li, S. Liu, J. Yang, Z. He, J. Zheng, Y. Li, Electrochemical methods contribute to the recycling and regeneration path of lithium-ion batteries, Energy Storage Mater. 55 (2023) 606–630, https://doi.org/10.1016/j.ensm.2022.12.022.
[7] T. Abbas, A. Ahmed Bazmi, A. Waheed Bhutto, G. Zahedi, Greener energy: issues and challenges for Pakistan-geothermal energy prospective, Renew. Sustain. Energy Rev. 31 (2014) 258–269, https://doi.org/10.1016/j.rser.2013.11.043.
[8] J. Son, K. Ma, Wind energy systems, Proc. IEEE 105 (2017) 2116–2131, https://doi.org/10.1109/JPROC.2017.2695485.
[9] L. Zhou, X. Li, G.W. Ni, S. Zhu, J. Zhu, The revival of thermal utilization from the Sun: interfacial solar vapor generation, Natl. Sci. Rev. 6 (2019) 562–578, https://doi.org/10.1093/nsr/nwz030.
[10] T. Kim, W. Song, D. Son, L. Ono, Y. Qi, Lithium-ion batteries: outlook on present, future, and hybridized technologies, J. Mater. Chem. A 7 (2019) 2942–2964, https://doi.org/10.1039/C8TA10513H.
[11] X. Lu, Z. Li, J. Zou, D. Peng, W. Hu, Y. Zhong, P. Li, S. Su, X. Wang, S. Wang, Z. Zhao, J. Zhang, Spent lithium manganate batteries for sustainable recycling: a review, Frontiers in Materials 10 (2023) 1152018, https://doi.org/10.3389/fmats.2023.1152018.
[12] Y. Li, W. Lv, H. Huang, W. Yan, X. Li, P. Ning, H. Cao, Z. Sun, Recycling of spent lithium-ion batteries in view of green chemistry, Green Chem. 23 (2021) 6139–6171, https://doi.org/10.1039/D1GC01639C.
[13] S. Kumawat, D. Singh, A. Saini, Recycling of spent lithium-iron phosphate batteries: toward closing the loop, Mater. Manuf. Process. 38 (2022) 135–150, https://doi.org/10.1080/10426914.2022.2136387.
[14] J. Tan, Z. Cheng, J. Zhang, X. Xiang, Nucleation–Oxidation coupled technology for High-Nickel ternary cathode recycling of spent Lithium-ion batteries, Sep. Purif. Technol. 298 (2022) 121569, https://doi.org/10.1016/j.seppur.2022.121569.
[15] J. Tan, Q. Wang, Y. Li, X. Xu, Direct preparation of battery-grade lithium carbonate via a nucleation–crystallization isolating process intensified by a micro-liquid film reactor, Can. J. Chem. Eng. 101 (2023) 13, https://doi.org/10.1002/cjce.24436.

[16] J. Kumar, R. Neiber, J. Park, R. Ali Soomro, G. Greene, S. Ali Mazari, H. Young Seo, J. Hong Lee, M. Shon, D. Wook Chang, K. Yong Cho, Recent progress in sustainable recycling of $LiFePO_4$-type lithium-ion batteries: strategies for highly selective lithium recovery, Chem. Eng. J. 431 (2022) 133993, https://doi.org/10.1016/j.cej.2021.133993.

[17] C. Liu, H. Ji, J. Liu, P. Liu, G. Zeng, X. Luo, Q. Guan, X. Mi, Y. Li, J. Zhang, Y. Tong, Z. Wang, S. Wu, An emission-free controlled potassium pyrosulfate roasting-assisted leaching process for selective lithium recycling from spent Li-ion batteries, Waste Manag. 153 (2022) 52–60, https://doi.org/10.1016/j.wasman.2022.08.021.

[18] D. Chang, S. Yang, P. Shi, Y. Jie, F. Hu, G. Fang, Y. Chen, Selective recovery of lithium and efficient leaching of transition metals from spent $LiNi_xCo_yMn_zO_2$ batteries based on a synergistic roasting process, Chem. Eng. J. 449 (2022) 137752, https://doi.org/10.1016/j.cej.2022.137752.

[19] Y. Tang, X. Qu, B. Zhang, Y. Zhao, H. Xie, J. Zhao, Z. Ning, P. Xing, H. Yin, Recycling of spent lithium nickel cobalt manganese oxides via a low-temperature ammonium sulfation roasting approach, J. Clean. Prod. 279 (2021) 123633, https://doi.org/10.1016/j.jclepro.2020.123633.

[20] C. Correa, C. de Santi, A. Leclerc, Green-PVC with full recycled industrial waste and renewably sourced content, J. Clean. Prod. 229 (2019) 1397–1411, https://doi.org/10.1016/j.jclepro.2019.04.383.

[21] L. Lu, W. Li, Y. Cheng, M. Liu, Chemical recycling technologies for PVC waste and PVC-containing plastic waste: a review, Waste Manag. 166 (2023) 245–258, https://doi.org/10.1016/j.wasman.2023.05.012.

[22] S. Mirkarimi, S. Bensaid, D. Chiaramonti, Conversion of mixed waste plastic into fuel for diesel engines through pyrolysis process: a review, Appl. Energy 327 (2022) 120040, https://doi.org/10.1016/j.apenergy.2022.120040.

[23] H. Pi, Y. Xiong, S. Guo, The kinetic studies of elimination of HCl during thermal decomposition of PVC in the presence of transition metal oxides, Polym.-Plast. Technol. Eng. 44 (2005) 275–288, https://doi.org/10.1081/PTE-200048727.

[24] L. Ciacci, F. Passarini, I. Vassura, The European PVC cycle: in-use stock and flows, Resources, Conserv. Recycl. 123 (2017) 108–116, https://doi.org/10.1016/j.resconrec.2016.08.008.

[25] E. Fan, L. Li, Z. Wang, J. Lin, Y. Huang, Y. Yao, R. Chen, F. Wu, Sustainable recycling technology for Li-ion batteries and beyond: challenges and future prospects, Chem. Rev. 120 (2020) 7020–7063, https://doi.org/10.1021/acs.chemrev.9b00535.

[26] J. Lin, L. Li, E. Fan, C. Liu, X. Zhang, H. Cao, Z. Sun, R. Chen, Conversion mechanisms of selective extraction of lithium from spent lithium-ion batteries by sulfation roasting, ACS Appl. Mater. Interfaces 12 (2020) 18482–18489, https://doi.org/10.1021/acsami.0c00420.

[27] H. Zhang, A. Tang, F. Luo, X. Xie, L. Yang, Y. Zheng, X. Tao, C. Qiu, C. Wang, A. Peng, X. Luo, P. Shao, Extraction of valuable metals from spent cathode materials by reductive roasting in methane atmosphere, Sep. Purif. Technol. 318 (2023) 123995, https://doi.org/10.1016/j.seppur.2023.123995.